Published in final edited form as:
J Neurochem. 2014 March ; 128(5): 686–700. doi:10.1111/jnc.12480.

KIBRA (KIdney/BRAin protein) regulates learning and memory and stabilizes Protein kinase Mζ

Angela Vogt-Eisele[*,1], **Carola Krüger**[*,1], **Kerstin Duning**[†,1], **Daniela Weber**[*,1], **Robert Spoelgen**[*], **Claudia Pitzer**[*], **Christian Plaas**[*], **Gisela Eisenhardt**[*], **Annette Meyer**[*], **Gerhard Vogt**[*], **Markus Krieger**[*], **Eva Handwerker**[*], **Dirk Oliver Wennmann**[†], **Thomas Weide**[†], **Boris V. Skryabin**[§,¶], **Matthias Klugmann**[**], **Hermann Pavenstädt**[†], **Matthew J. Huentelmann**[‡], **Joachim Kremerskothen**[†], and **Armin Schneider**[*]

[*]SYGNIS Bioscience, 69120 Heidelberg, Germany

[†]Department of Internal Medicine D, General Internal Medicine and Nephrology, University Hospital of Münster, 48149 Münster, Germany

[‡]The Translational Genomics Research Institute, Neurogenomics Division, Phoenix, AZ 85004, USA

[§]Institute of Experimental Pathology, ZMBE, University of Münster, Von-Esmarch-Str. 56, 48149 Muenster, Germany

[¶]Interdisciplinary Center for Clinical Research (IZKF), University of Muenster, 48149 Muenster, Germany

[**]Dept. Functional Genomics, University of New-South Wales, Sydney, NSW 2052, Australia

Abstract

The WWC1 gene has been genetically associated with human episodic memory performance, and its product KIBRA has been shown to interact with the atypical protein kinase PKMζ. Although recently challenged, PKMζ remains a candidate postsynaptic regulator of memory maintenance. Here we show that PKMζ is subject to rapid proteasomal degradation and that KIBRA is both necessary and sufficient to counteract this process, thus stabilizing the kinase and maintaining its function for a prolonged time. We define the binding sequence on KIBRA, a short amino acid motif near the C-terminus. Both hippocampal knock-down of KIBRA in rats and KIBRA knock-out in mice result in decreased learning and memory performance in spatial memory tasks supporting the notion that KIBRA is a player in episodic memory. Interestingly, decreased memory performance is accompanied by decreased PKMζ protein levels. We speculate that the stabilization of synaptic PKMζ protein levels by KIBRA may be one mechanism by which KIBRA acts in memory maintenance.

Keywords

Memory; proteasome; degradation; kinase; ubiquitin; protein-protein interaction; hippocampus; knock-out; postsynaptic density

KIBRA (kidney/brain) protein encoded by the human WWC1 (WW and C2 domain containing 1) gene has been implicated in human episodic memory performance by multiple

Address correspondence and reprint requests to Armin Schneider, SYGNIS Bioscience, 69120 Heidelberg, Germany. schneider@sygnis.de.
[1]These authors contributed equally to the work.

genome-wide association studies (Papassotiropoulos *et al.* 2006, Schneider *et al.* 2010, Milnik *et al.* 2012). This function appears biologically plausible as KIBRA interacts with synaptic proteins (Büther *et al.* 2004), localizes to the postsynaptic density (Johannsen *et al.* 2008), and is expressed in brain regions involved in learning and memory, i.e. hippocampus and cortex (Johannsen et al. 2008). However, the most intriguing biochemical link to memory performance consists in the association of KIBRA with the brain-specific protein kinase M ζ (PKMζ) (Yoshihama *et al.* 2009, Büther et al. 2004), a molecule involved in memory maintenance (Sacktor 2008, Sacktor *et al.* 1993, Shema *et al.* 2007, Shema *et al.* 2011). PKMζ mRNA is stored in dendrites and only translated locally after sufficient synaptic stimulation (Osten *et al.* 1996, Muslimov *et al.* 2004). These transcripts are generated by an independent promoter within the protein kinase C ζ (PKCζ) gene, such that the resulting PKMζ protein is identical to the carboxyterminal catalytic domain of PKCζ while lacking the aminoterminal autoinhibitory domain of PKCζ (Hernandez *et al.* 2003). This structural feature results in constitutive and persistent PKMζ activity after initial kinase activation via phosphorylation by the phosphoinositide-dependent kinase 1 (Kelly *et al.* 2007), and experimental inhibition of synaptic PKMζ activity efficiently erases even well-consolidated memories (Migues *et al.* 2010, for review see Sacktor 2010). Recently the role of PKMζ in memory maintenance has been challenged by the analysis of knock-out mice, and by questions regarding the specificity of the inhibitory ZIP peptide used in several studies (Lee *et al.* , Volk *et al.* , Lisman 2011).

Here we show that PKMζ undergoes rapid turnover via proteasomal degradation under basal conditions, and that KIBRA counteracts this degradation to facilitate accumulation of the kinase. Strikingly, ablation or reduction of KIBRA expression in vivo selectively reduces hippocampal PKMζ protein levels and impairs spatial memory performance in both rats and mice. We propose that both KIBRA and PKMζ are important elements of memory maintenance that act along the same pathway.

Materials and Methods

Plasmids and Constructs

All expression plasmids were constructed by Gateway cloning (Invitrogen, Carlsbad, CA) and point mutations were introduced by site-directed mutagenesis. The human ubiquitin ORF was purchased from Invitrogen as an Entry clone and was recombined with the respective DEST vector to obtain a V5-tagged Ubiquitin expression plasmid. EYFP-fusions of KIBRA-fragments from the PKMζ binding region were generated by alignment of oligonucleotides and ligation into an EcoRI and XhoI-digested pEYFP-C1 (Clontech, Mountain View, CA) vector. A detailed list of oligonucleotides used for cloning constructs used in the interaction site mapping experiment is given in Supporting information 11.

AAV expression constructs and generation of AAV 1/2 virus

Vectors intended for shRNA expression were based on the AAV2 ITR-flanked shRNA expression cassette pAM/U6-pl-CBA-hrGFP-WPRE-BGHpA described earlier (Franich *et al.* 2008), which facilitates humanized renilla GFP reporter gene expression from a CBA hybrid promoter along with shRNA expression from a RNA polymerase III compatible human U6 promoter. For knock-down of KIBRA transcript levels, a target sequence at position 1276 of the KIBRA ORF (GAT CCG TTG AAG TTA AAC AGC AAG ATT CAA GAG ATC TTG CTG TTT AAC TTC AAC CTT TTT TGG AAA) was identified with Invitrogen's BLOCK-iT™ RNAi Designer web tool, and complementary DNA oligonucleotides encoding a shRNA directed against this target sequence were generated using Ambion's pSilencer™ Expression Vectors Insert Design Tool. For the loop structure, the sequence GTG AAG CCA CAG ATG was used as described previously (Zeng & Cullen

2004). Annealed oligos were then BamHI/ HindIII subcloned into the polylinker site. The resulting vector was termed AAV-(rat)-KIBRA-RNAi. AAV-eGFP was used as control vector. Generation of AAV-eGFP was performed by subcloning the coding sequence of eGFP into the AAV2 backbone plasmid containing the chicken β-actin promoter and an IRES-eGFP sequence, flanked by AAV2 ITR sequences. HEK293 cells were used for the production of pseudotyped chimeric AAV1/2 vectors (containing a 1:1 ratio of capsid proteins serotype 1 and 2) as described previously (Klugmann *et al.* 2005). Cultured cells (80% confluent) propagated in complete DMEM were transfected with the AAV construct and helper plasmids (pH21, pRV1 and pFΔ6) by calcium phosphate transfection. 48 h later, cells were harvested in PBS, centrifuged, and pellets from 5 plates were pooled in 25 ml of a buffer consisting of 150 mM NaCl, 20 mM Tris pH8, 1.25 ml of 10% Natriumdeoxycholate and 50 U/ml of benzonase. After an incubation of 1 h at 37°C, 25 ml of 150 ml NaCl and 1.25 ml of 10% Natirumdeoxycholate were added and the solution was centrifuged. The supernatant was collected and filtered with 450 mM NaCl, 20 mM Tris (pH 8) through a high affinity heparin column (1 ml HiTrap Heparin, Sigma) previously equilibrated with buffer (150 mM NaCl, 20 mM Tris pH 8), at a speed of 1 ml/min. The genomic titre of the viral solutions was determined by real-time PCR (Roche Diagnostics, Mannheim, Germany).

Stereotactic injection

AAV vectors were injected bilaterally into the adult hippocampus at 4 sites per hemisphere. For each hemisphere, a total volume of 4 μl was injected of a virus solution containing 7×10^9 virus particles/ ml. The coordinates used for each hemisphere were 1) AP 5.8 mm from the lambda; ML 1.0 mm from the sagittal suture and DV 4.2 mm from the bregma, 2) AP 4.4 mm from the lambda; ML 2.9 mm from the sagittal suture and DV 3.9 mm from the bregma, 3) AP 3.8 mm from the lambda; ML 4.0 mm from the sagittal suture and DV 3.8 mm from the bregma, 4) AP 3.2 mm from the lambda; ML 4.6 mm from the sagittal suture and DV 6.2 mm from the bregma. Vector delivery was performed with a microprocessor-controlled minipump (World Precision Instruments, Sarasota, FA, USA) with 34×G beveled needles (World Instruments) in a stereotaxic frame (Kopf Instruments, Tujunga, CA, USA). One group (n=19) received the KIBRA knock down virus, control rats (n=20) were injected with equivalent volumes of AAV-eGFP.

BiFC analysis

HeLa cells were grown in Dulbecco's modified Eagle's medium (DMEM) supplemented with 10% FCS at 37 °C in 5% CO_2/95% O_2. Cells were transiently transfected with plasmids using Lipofectamine2000 (Invitrogen, Carlsbad, CA) according to the manufacturer's instructions. The constructs pVen1 and pVen2 encoding the N-terminus (aa 1-154) and C-terminus (aa 155-238) of the Venus protein, respectively were a kind gift from M. Hatzfeld (University of Halle, Germany). For the BiFC experiments, KIBRA and PKMζ cDNA were cloned into pVen1 and pVen2, respectively. HeLa cells were cotransfected either with pVen1 or with pVen1-KIBRA in combination with pVen2-PKMζ. After 24 h, cells were fixed and the actin cytoskeleton was labeled with Alexa594-conjugated phalloidin. Fluorescence images were taken using an upright Axioscope microscope (Zeiss, Jena, Germany) equipped with a Zeiss CCD camera. Image data were analyzed using Axiovision software (Zeiss, Jena, Germany) and Adobe Photoshop software (Adobe Systems, San Jose, CA, USA).

Western blotting

Cells were washed once with icecold PBS and scraped off the plate after adding Lysis buffer (50 mM Tris/HCl pH 7.4, 150 mM NaCl, 1 mM EDTA, 1% NP40, 0.2 mM PMSF, Protease

Inhibitor Cocktail (Roche Diagnostics, Mannheim, Germany)). Lysates were frozen in liquid nitrogen and stored afterwards at -20°C. After syringing the lysate 5×, lysate was spun down at 13000 rpm at 4 °C for 10 min and the protein concentration of the supernate was determined (BCA-Test, Pierce/Thermo Fisher Scientific, Bonn, Germany). 1/5 volume of 5× sample-buffer (with β-Mercaptoethanol) was added and samples were denatured at 95 °C for 5 min. 50 μg of protein was run on a SDS-PAGE and proteins were transferred to nitrocellulose membranes using an iBlot™ Dry Blotting System (Invitrogen, Karlsruhe, Germany). Blots were blocked with 5% milk powder in PBS/0.2% Tween20, washed three times with PBS/0.2% Tween20, and incubated with the primary antibody (anti-flag 1:10000, mouse monoclonal (Sigma, Taufkirchen, Germany); anti-V5 1:5000, mouse monoclonal (Sigma, Taufkirchen, Germany); anti-Rock1 1:250, rabbit polyclonal, CellSignaling (NEB, Frankfurt, Germany); anti-Rock2 1:1000, rabbit polyclonal, CellSignaling (NEB, Frankfurt, Germany); anti- p190 RhoAGAP 1:1000, rabbit polyclonal, CellSignaling (NEB, Frankfurt, Germany); anti-CamKII, 1:500 rabbit polyclonal, CellSignaling (NEB, Frankfurt, Germany); anti-RhoA (67B9) 1:1000, rabbit polyclonal, CellSignaling (NEB, Frankfurt, Germany); anti-Actin 1:10 000, mouse monoclonal (Millipore, Schwalbach, Germany); anti-PKCζ (C-20) 1:200, rabbit polyclonal (Santa Cruz, Heidelberg, Germany); p-PKCζ-T410 1:200, rabbit polyclonal (Santa Cruz, Heidelberg, Germany); anti-PDK1 1:1000 (Cell Signaling, Frankfurt, Germany) over night at 4°C. After washing, the blots were incubated with the secondary antibody (anti-rabbit- or anti-mouse-HRP-conjugated-antiserum) for 1 h at room temperature. Signals were detected using the supersignal chemiluminescence system (Pierce, Rockford, IL, USA) and exposed to CL-Xposure film (Pierce). For quantification of scanned autoradiographs Windows ImageJ (NIH, Bethesda, MD,USA) was used.

For analysis of brain extracts, animals were sacrificed at the indicated time points. Animals were deeply anesthetized with ketamine/xylazine, and perfused transcardially with Hank's balanced salt solution (HBSS). For this, the thorax was opened, and the right ventricle punctured a 21G cannula. The brain was immediately dissected, and the hippocampi prepared on ice using a stereomicroscope. Hippocampi were snap-frozen on dry ice and stored at -80 °C. For protein extraction, 500 μl protein extraction buffer (containing 50 mM Tris-HCl pH 8, 10 mM EDTA, PMSF (1:1000), and 1× complete protease inhibitor cocktail (Roche Diagnostics, Mannheim, Germany) was used per rat hippocampus. The tissue was minced with an ultraturrax, and put immediately on ice. SDS was added to a final concentration of 2%. The solution was then treated by ultrasound 2-3 times. Benzonase (Sigma, Taufkirchen, Germany) and MgCl2 were added, and incubated for 1 h at 4°C. The sample was then centrifuged for 10 min at app. 17000 g, and 1 μl of the supernatant used for protein quantification. Western blots were run and immunostaining performed as described above.

Kinase assays

CREB phosphorylation assays were performed using the SignaTECT Protein Kinase C Assay System from Promega and ^{33}P γATP (10 μCi/μl) provided by Perkin Elmer following the manufacturer's instructions. Briefly, after expression in COS1 cells with or without co-expression of KIBRA, Flag-tagged PKCζ was harvested as described under “Co-Immunoprecipitation” in lysis-buffer containing 1% NP40. Harvested protein samples were quantified by Western blotting, and equal amounts were applied in the phosphorylation assay. Bead suspensions were diluted 1:2 in 0.1 mg/ml BSA/0.05% Triton. 5 μl of bead-coupled protein or 9 ng of recombinant PKCζ provided by Upstate/Millipore (positive control) and added to 20 μl PKC reaction mix containing 1× PKC activation buffer, 1.2 μM biotinylated CREB peptide substrate, 0.1 mM ATP and 1 μM ^{33}P γATP (1 μCi/sample). Samples were incubated for 5 minutes at 30°C. The reaction was stopped with termination buffer as supplied and 10 μl of terminated reactions were spotted onto the SAM membrane.

Membranes were washed as described in 200 mM NaCl and 2 M NaCl/1% H_3PO_4 and distilled water. Analysis was performed by phosphoimaging (Fuji scanner FLA 2000).

Quantitative PCR

KIBRA-overexpressing primary neuronal cells were harvested 5 d after transduction of KIBRA by AAV for RNA preparation using the Qiagen RNeasy Mini Kit (Qiagen, Hilden, Germany) following the manufacturers recommendations. cDNA was synthesized from 2 μg total RNA using oligo-dT primers and superscript II reverse transcriptase (Invitrogen, Karlsruhe, Germany) according to standard protocols. Quantitative RT-PCR was performed using the Lightcycler system (Roche Diagnostics, Mannheim, Germany) with SYBR-Green staining of doublestranded DNA. The following primer pairs were used: KIBRA sp-1 2982mm “GAA GGA GCT GAA GGA GCA TTT”, KIBRA asp-1 3219mm “CCT GAA AGA CTG CAC TTC TGG”; PKCζ 5′fwd “CGC TCAC CCTC AAG TGG GTG GAC AG”, PKCζ and PKMζ 3′rev “GGC TTG GAA GAG GTG GCC GTT GG”; PKMζ 5′fwd “CCA CCC GGG CCT GGA GAC ATG”. Cycling conditions were as follows: 10min at 95°C; 5s at 95°C, 10s at 60°C, 30s at 72°C, and 10s at 84 for 45 cycles for KIBRA, and 10min at 95°C; 5s at 95°C, 10s at 67°C, 30s at 72°C, and 10 s at 83 for 45 cycles for PKC/Mζ. Melting curves were determined using the following parameters: 95 °C cooling to 50 °C; ramping to 99 °C at 0.2 °C/sec. Specificity of product was ensured by melting point analysis and agarose gel electrophoresis. cDNA content of samples was normalized to the expression level of Cyclophilin (primers: „cyc5“ ACC CCA CCG TGT TCT TCG AC; „acyc300“ CAT TTG CCA TGG ACA AGA TG). Relative regulation levels were derived after normalization to native cortical neurons.

Proteasome activity assay

For assaying the influence of KIBRA on proteasome activity in COS1 cells, a 20S Proteasome activity assay (#APT280, Millipore, Germany) was used. In this assay, a labeled substrate (LLVY-7-Amino-4-methylcoumarin (AMC)) is cleaved and fluorescence of the free AMC fluorophore can be quantified using a 380/460 nm filter set. COS1 cells were transfected with pExp_nV5_KIBRA_hu, pExp_NterFlag_PKMzeta_hu or with the respective V5-/Flag- control-plasmids. 2d after transfection, cells were harvested for the assay using a lysis-buffer containing 50 mM HEPES (pH 7.5), 5 mM EDTA, 150 mM NaCl and 1% Triton X-100. Cell extraction and proteasome activity assay were performed according to the manufacturer's instructions, including a proteasome positive control and Lactacystin as proteasome inhibitor. Fluorescence data was collected by using a BMG FLUOstar plate reader (BMG, Ortenberg, Germany) using 340 nm excitation and 450 nm emission filters.

Animals

In these studies, male Wistar rats (250 g body weight) and KIBRA knock-out mice (see section “KIBRA knock-out mice”) were used. All animals were housed at constant temperature (23° C) and relative humidity (60%) with a fixed 12 h light/dark cycle. Food and water were accessible *ad libitum* except for transient food restrictions for rats undergoing 8-arm maze testing (see section “Behavioural testing”). All animal experiments were conducted in a fully blinded and randomized fashion and were approved by the responsible authority (Regierungspräsidium Karlsruhe, Germany). Reporting of the animal experiments in the paper adheres to the ARRIVE guidelines (Kilkenny *et al.* 2011, Kilkenny *et al.* 2010).

KIBRA knock-out mice

To generate floxed KIBRA mice, we used a gene targeting strategy (targeting vector pK15-KIBRA) using two loxP sites flanking exon 15 which codes for the C2 domain of the KIBRA. Targeted mouse embryonic stem cells (CV19) were injected to C57Bl/6xDBA blastocysts and implanted in pseudo pregnant CD1 females to generate chimeric offspring. After successful germ line transmission, mice were crossed with phosphoglycerate kinase (PGK)-driven Cre deleter mice to obtain ubiquitous *in vivo* KIBRA deletion (Lallemand et al., 1998). Wildtype and knock-out mice were of the 129SV/C57BL6 hybrid background backcrossed three times to C57Bl6/N (Jackson Labs).

Behavioural testing

Open field—The open field consists of an opaque PVC box (90×90×90 cm). To evaluate locomotor activity the arena was divided into 4×4 equal squares and the 4 inner squares were defined as the center region. Animals were introduced to the box in the lower right corner facing the wall and left to freely explore for 5 min. Animals were tracked using SYGNIS Tracker software.

Morris water maze (MWM)—A circular pool (diameter 1.70 m) was filled with water to a height of 30 cm. Non-toxic colour was added to the water to prevent visual access of animals to a platform submerged 1 cm below the water surface in the centre of the north-west (NW) quadrant of the pool. Distal visual cues were placed in the surrounding of the arena to facilitate spatial orientation for the rats. Animals were tracked via a top-mounted camera connected to SYGNIS tracker software. A non-spatial pre-training session using a visible platform was performed to habituate animals to the maze. During this session, the pool was shielded from extra-maze cues by black curtains to prevent acquisition of spatial information. Spatial training consisted of five days with four daily trials and a cut-off time of 60 s each. Animals were released from the SW, S, SO and O points of the pool in a balanced pseudo randomized manner such that the start point frequency and the distance to the platform were distributed equally across the test. After climbing onto the platform, rats were allowed to remain on the platform for 30 s before being returned to the cage for a 5 min intertrial interval. Rats failing to locate the platform were guided to the target and were allowed to remain there for 30 s. On the fifth day, animals were subjected to a probe trial in which the platform was removed. Animals were allowed to search for the platform for 120 s.

Radial 8-arm maze—The maze consisted of 8 arms radiating equally spaced from a central platform. Four arms contained a food pellet at their distal end (baited arms) and four were empty (unbaited arms). For this test, animals were transiently food deprived and maintained at 90% of their free-feeding weight. The central platform was 25 cm in diameter and each arm measured 50 cm × 10 cm. Walls consisted of transparent walls 20 cm high. Rats were randomly introduced to unbaited arms (random start arm) and were allowed to enter baited arms to pick up the pellets. Animals acquire both a working and a reference memory relating to arms already entered in the present trial and to previously unbaited arms, respectively. Three daily trials of 5 minutes each were conducted for 3 consecutive weeks (15 days). Animals were tracked using SYGNIS tracker software.

Active place avoidance—The active place avoidance apparatus (Serrano *et al.* 2008) was located in a testing cubicle with visual cues on the inside walls. It consisted of a slowly rotating (1 rpm) circular platform (r = 40 cm) surrounded by a transparent wall. One randomly chosen 60° sector of the arena was designated as the non-rotating shock zone where animals received a mild 0.4 mA electric shock upon entry, and further identical shocks every 1.5 s if they failed to leave the sector. The shock zone was identical for all animals and its location only identifiable relative to the extra-maze visual cues. Due to

platform rotation, any passive strategy was inevitably associated with foot-shocks, and animals quickly learned to actively avoid the shock zone. After a 10 min pre-training trial without shocks, 9 training trials of 10 min each were conducted at inter-trial intervals of 12 min which animals spent in their home cages. After 24 hours, one retention trial was run without triggering foot shocks. Latency to shock zone entry and time spent in that sector were recorded during all trials.

Co-immunoprecipitation

Two days after electroporation, COS1 cells were washed twice with ice-cold PBS and followed by lysis at 4 °C for protein extraction. Lysis buffer contained 50 mM Tris/HCl pH 7.4, 150 mM NaCl, 0.5% NP40, 20 mM NaF, 2 mM EDTA, 2 mM EGTA, 2 mM Orthovanadate, protease inhibitor cocktail. After incubation for 20 min at 4°C, lysate was spun down at 13500 rpm at 4 °C for 10 min. One part of the supernatant was kept for direct Western analysis (Lysate). The other part was incubated with anti-flag beads (anti-Flag M2 Affinity Gel, Sigma, Taufkirchen, Germany) at 4 °C for 2 h. After precipitation of the anti-flag-antigen-complex, beads were washed three times with TBS (50 mM Tris/HCl, 150 mM NaCl). To release the flag-bound-complex from the beads, SDS loading buffer (without reducing reagents) was added and incubated at 95°C for 5 min. After spinning down the beads, supernatant (IP) was analysed by performing SDS-PAGE and transferring proteins onto nitrocellulose membranes (iBlot™ Dry Blotting System, Invitrogen, Carlsbad, CA, USA). Blots were blocked with 5% milk powder and incubated overnight at 4 °C with the primary antibody (anti-flag M2 Monoclonal Antibody, 1:10000 (Sigma, Taufkirchen, Germany) and anti-V5 Antibody, 1:5000 (Sigma, Taufkirchen, Germany), respectively). After washing, the blots were incubated with the secondary antibody (anti-mouse antiserum HRP-coupled, 1:8000 (Dianova, Hamburg, Germany) for 1 h at room temperature. Signals were detected using the supersignal chemiluminescence system (Pierce, Rockford, IL, USA) and exposed to CL-Xposure film (Pierce, Rockford, IL, USA).

Statistics

Two and more group comparisons were done using t-test or ANOVA, respectively. Time series were analyzed using regression analyses. Analyses were done with JMP 9.02 (SAS Institute), and p-values < 0.05 were considered significant.

Results

We confirmed interaction of PKMζ with KIBRA in co-transfected COS1 cells by co-immunoprecipitation (Fig. 1A). The binding was very robust and reproducible under multiple lysis conditions and detergents (data not shown). To confirm an interaction of KIBRA and PKMζ in a cellular environment we used bimolecular fluorescence complementation (BiFC) analysis. Co-expression of KIBRA fused to the N-terminus of the Venus protein together with a fusion protein containing PKMζ and the Venus C-terminus revealed strong, aggregate-like BiFC signals in the cytosol of transfected HeLa cells indicating direct interaction of the two proteins (Fig. 1B, lower panel) while only faint background signals were seen when the Venus N-terminus alone was expressed in the presence of the C-terminal Venus-PKMζ fusion protein (Fig. 1B, upper panel). We have previously demonstrated that PKMζ can phosphorylate two serine residues (S975 and S978) near the human KIBRA C-terminus (Büther et al. 2004). Mutating those residues to alanine or glutamate had no influence on the interaction observed (Supporting information 1). The stability of this interaction and the absence of any influence of S975/S978 phosphorylation in KIBRA suggest that this is not of a typical kinase-target interaction.

During co-expression experiments in COS1 cells we noted that PKMζ protein levels increased strongly in the presence of KIBRA (Fig. 1C). This effect appeared specific as the levels of a number of other protein kinases were not affected by co-overexpression with KIBRA in COS1 cells (Fig. 1D). Moreover, PKMζ levels correlated to KIBRA input amounts in an approximately linear relationship (Fig. 1E).

We next monitored the influence of KIBRA overexpression on PKMζ and PKCζ mRNA levels to analyze a possible role for KIBRA in regulation of transcriptional activity or mRNA stability. However, endogenous PKCζ and PKMζ mRNA levels were not influenced by increased levels of KIBRA in primary cortical neurons (Fig. 2A). This effect could also be confirmed in other cell lines overexpressing PKMζ under a heterologous promoter (data not shown), suggesting that neither endogenous promoter activity nor mRNA stability are targeted by KIBRA. We therefore asked whether KIBRA stabilizes PKMζ on the protein level. Treatment of PKMζ-transfected COS1 cells with the protein translation inhibitor cycloheximide (CHX) led to a rapid decrease of PKMζ protein levels within 48 h. In contrast, concomitant overexpression of KIBRA stabilized PKMζ levels suggesting that KIBRA interferes with kinase degradation (Fig. 2B). PKMζ degradation appeared proteasome-mediated as the proteasome inhibitor MG-132 efficiently prevented the time-dependent decrease in PKMζ levels in the presence of cycloheximide (Fig. 2C), while lysosomal inhibitors had no such effect (data not shown). These data could be confirmed in a number of other cell types, e.g. the neuronal SHSY-5Y cell line (Supporting information 2). Importantly, KIBRA did not affect general proteasome activity as judged by a fluorescence-based proteasome activity assay (Fig. 2D). As further evidence for a proteasomal pathway-mediated degradation of PKMζ, the kinase was ubiquitinylated in COS1 cells co-transfected with V5-ubiquitin and PKMζ (Fig. 2E), and by endogenous ubiquitin in the presence of MG-132 (Fig. 2F). Interestingly, it has been recently reported that KIBRA also shields PKMζ-related kinases LATS 1, LATS 2, and AGC (protein kinase A, G, and C families) from proteasomal degradation (Xiao *et al.* 2011).

In contrast to PKCζ, which contains an autoinhibitory domain, PKMζ is constitutively active after initial phosphorylation by PDK1 with PDK1 being sufficient for PKMζ activation (Kelly et al. 2007). The constitutive kinase activity of PKMζ is thought to be crucial in its role in maintaining long-term memory storage (Sacktor 2008). We therefore asked whether binding of KIBRA to PKMζ is dependent on the activation state of the kinase. Indeed, the PKMζ co-immunoprecipitated with KIBRA from double-transfected COS1 cells was phosphorylated at the activation loop threonine 227, thus indicating an activated state of the kinase (Fig. 3A). Next we determined kinase activity of both free and KIBRA-bound PKMζ after immunoprecipitation from COS1 cells. CREB target peptide phosphorylation was determined by a radioactive filter assay in comparison to in vitro-synthesized and purified PKCζ. Equal amounts of PKMζ as determined by Western blot were entered into the assay. Presence of KIBRA did not alter the kinase activity of PKMζ (Fig. 3B). As PKMζ bound to KIBRA was phosphorylated by PDK1 at T227, we asked whether PDK1 also binds KIBRA or remains bound to PKMζ after phosphorylation. This was not the case as shown by co-immunoprecipitation after co-expressing KIBRA and PKMζ and detecting endogenous PDK1 (Fig. 3C). We next determined whether KIBRA was able to bind non-active forms of PKMζ. These analyses revealed that KIBRA binding was abolished by any of the following three alanine mutations: critical activation loop threonine 227 corresponding to position 410 in PKCζ (Le Good *et al.* 1998); the turn-motif autophosphorylation site threonine 377 corresponding to threonine 560 in PKCζ; glutamate 396 corresponding to glutamate 579 within the hydrophobic PDK1 docking site motif PKCζ (Fig. 3D). Notably, basal expression of the mutant kinases was very weak, suggesting that inactive PKMζ is subject to enhanced degradation. Mutating the highly conserved lysine residue responsible for orientation of the α- and β–phosphates of ATP (K98W), and essential for kinase activity also resulted in a

highly unstable protein that did not bind KIBRA (Fig. 3E). Deleting the carboxyterminus of the kinase (Δ371-409) containing the hydrophobic motif (392-397) necessary for initial PDK1 docking (Balendran *et al.* 2000) fully abolished KIBRA binding (Fig. 3F). Finally, in an in vitro interaction study where both proteins were expressed separately, dephosphorylating PKMζ interfered with binding (Fig. 3G). We therefore propose that previous activation of PKMζ by PDK1 is essential for KIBRA to bind and protect PKMζ from degradation and that KIBRA-bound kinase retains its activity.

We next determined the binding motif(s) in KIBRA responsible for binding. By deletion series we determined that a region in the C-terminal third was necessary for binding (data not shown). Fine deletion mapping indicated amino acids 946 – 985 as essential (Fig. 4A). EGFP-fusion of different stretches within that region indicated a 20 amino acid motif (PPFVRNSLERRSVRMKRPSS (aa 956 – 975)) necessary and sufficient for PKMζ binding (Fig. 4B). Further deletion mapping indicates that the absolute minimal binding motif ranges from position 958 to 970, however, with a loss of binding activity compared to the 20mer sequence (Fig. 4C). An alanine scan from position 964 to 974 showed that the arginine at position 965 is indispensable for binding within the binding motif, while all other single point mutants retained binding activity, with a decrease both for the S967A and R969A positions (Fig. 4D; see Supporting Information 3 for full scan). A synthetic peptide containing the binding motif (from aa 948-978) was sufficient for binding (Fig. 4E), and able to displace KIBRA from a pre-formed complex with PKMζ in a concentration-dependent manner (Fig. 4F). These positive binding experiments with a minimal motif also rule out that failure of binding in the deletion mutants was due to misfolding rather than to the absence of the binding motif. Finally, different cell-penetration peptide (CPP) motifs were fused to our core peptide and were able to bind to PKMζ inside cells as shown by co-immunoprecipitation with streptavidin to capture the biotinylated peptides that had penetrated into the cells (Fig. 4G). Most importantly, co-expressing the EGFP-peptide-fusion construct with PKMζ was sufficient for stabilization of the kinase (Fig. 4H).

We then studied consequences of reduced or absent KIBRA expression in rodent models on learning and memory performance. Knocking down KIBRA expression in the rat hippocampus by AAV-mediated siRNA delivery resulted in a reduction of KIBRA expression by 60% on the protein level (Fig. 5A; see also Supporting Information 4 for in vitro efficacy of the chosen siRNA). An initial open field test revealed no significant differences between siRNA-treated and control animals in parameters such as overall distance travelled, mean velocity, or time or distance spent in center (Supporting Information 5). In the Morris water maze, the acquisition phase over 16 trials using random choices of 4 start positions yielded similar performances of both groups with a slight disadvantage for the siRNA group that resulted in comparable latency times reached at trial 16 (Fig. 5B). However, as shown in Fig. 5C, in the recall trial animals with down regulated KIBRA levels in the hippocampus spent significantly less time in both the former platform location proper ($p<0.05$) and the extended target area defined as a circle around the former platform center with a radius four times as large as that of the platform ($p<0.05$). These results are also visualized as a heat map for location probability (Fig. 5C). Additionally, inferior recall of the platform location in knock-down animals 24 h after training was also evidenced by an increase in cumulative distance to the platform location (data not shown, $p<0.05$). As a non-aversive learning paradigm we chose the radial 8-arm maze. Compared to controls, AAV-siRNA-treated rats displayed more errors in both working memory ($p<0.05$, Fig. 5D) and reference memory ($p<0.05$, Fig. 5E). While for working memory errors only the offset difference between the error curves was significantly altered, there was a true slope difference for reference memory acquisition ($p<0.05$ by regression analysis).

Conditional KIBRA knock-out mice were generated, and crossed to PGK-Cre expressing animals resulting in complete absence of KIBRA expression in the brain (Supporting Information 6). These mice showed no gross anatomical or behavioral deficit, and behaved indistinguishably from their wild type littermates in parameters like exploratory drive, motor behavior, and anxiety as judged by an open field experiment (Supporting Information 7). We measured spatial memory performance in those animals by using an active place avoidance paradigm where mice were trained to avoid a predefined sector of a rotating disc. Ablation of KIBRA resulted in significantly inferior acquisition performance of the task (Fig. 6A), and in a reduced recall performance 24 h later (Fig. 6B both delay and time $p<0.05$). Importantly, recall was impaired by absence of KIBRA independently of the previous acquisition deficit ($p<0.05$ for factor genotype). In conclusion, reduction of KIBRA levels or absence of the protein impairs spatial learning and memory performance.

Based on our finding that PKMζ is stabilized by KIBRA in cell culture, we determined hippocampal PKMζ levels in our rodent models where KIBRA was down regulated or absent. Notably, PKMζ levels were decreased by more than 50% in the hippocampi of rats treated with KIBRA siRNA compared to controls, and by more than 60% in the knock-out mice (Fig. 6C). These data indicate that KIBRA's protective effect on PKMζ protein is also active in the functioning brain. Finally, we sought to determine whether viral delivery of a PKMζ-binding peptide EGFP fusion protein in rats could also influence PKMζ levels. This approach led to protection of endogenous PKMζ in primary cortical neurons (Supporting Information 8). In vivo, PKMζ levels were increased by more than 2.5-fold compared to EGFP wild type and a virus delivering the non-binding point mutant (Fig. 6D). Learning and memory performance in rats that had received the wt peptide-EGFP fusion also were clearly enhanced although this did not reach statistical significance due to the low number of animal used in this experiment and the principally increased difficulty to detect enhanced memory performance versus healthy controls (Supporting Information 9).

Discussion

Here we have demonstrated that 1.) reducing KIBRA levels leads to decreased learning and memory performance in spatial memory tasks, 2.) KIBRA levels correlate strongly to PKMζ protein levels, and 3.) PKMζ is degraded by the proteasome, and this process is inhibited by direct interaction between a short sequence motif near the C-terminus of KIBRA and the kinase. In vivo consequences of altering KIBRA levels have been examined by knock-down, by gene silencing, and by viral overexpression of a binding motif EGFP fusion protein. In the knock-down experiment an alternative to EGFP only as control could have been the use of a non-specific shRNA that does not target any gene in the genome to control against possible general off-target effects of shRNAs. In the context of the other experimental in vivo data this theoretical caveat does however not compromise the overall conclusion.

Our data about the role of KIBRA in synaptic plasticity and memory formation are further supported by a recent report that KIBRA deficiency in mice alters AMPA-receptor trafficking through an interaction with protein-interacting-with-kinase-1 (PICK1), interferes with long-term potentiation, and leads to inferior memory performance in a fear conditioning experiment (Makuch *et al.* 2011). Of note, PKMζ is also thought to ultimately act through AMPA receptor cycling upstream of PICK1 (Migues et al. 2010, Yao *et al.* 2008, Sacktor 2011). It is therefore tempting to speculate that these two mechanisms finally converge in the interaction of KIBRA and PKMζ, and the controlled lifetime of the kinase. It will be interesting to see whether KIBRA exerts a similar role for other PKC family members such as PKCα or ε that have also been implied in memory processes (e.g. (Hongpaisan *et al.* 2013).

Recently analyses of PKMζ knock-out mice have shown, that presence of PKMζ is not an absolute requirement for memory maintenance (Volk et al. 2013, Lee et al. 2013). Also recently, the specificity of the inhibitory ZIP peptide for PKMζ used as a tool in many functional studies has been doubted (Lisman 2011). However, several studies on PKMζ function have used genetic manipulation, especially overexpression, instead of the ZIP peptide, and the knock-out studies cannot rule out compensatory mechanisms. Therefore, although PKMζ does not appear to be the only and necessary regulator of memory maintenance, the broad evidence for a role of PKMζ in memory suggests that it may be one among several mechanisms at least in wild type mice that contribute to memory maintenance (discussed in more detail in (Glanzman 2013, Frankland & Josselyn 2013)). We have not generated any data in the paper that address the role of PKMζ independent of KIBRA manipulations, and can therefore not comment on the function of PKMζ in memory from own experimental evidence. However, in all our experiments there is a striking correlation between PKMζ levels and memory performance. We believe that PKMζ is one contributor to memory maintenance, and likely one of the pathways by which KIBRA exerts its effects on memory. Possibly the mechanisms exerted by KIBRA on PKMζ could also apply to other kinases relevant for memory, especially other kinases of the PKC family.

A tentative model for KIBRA's function in memory under the hypothesis that PKMζ is one player in synaptic maintenance could be the following: PKMζ is rapidly degraded after local dendritic synthesis unless KIBRA is available for binding and preservation of the kinase. It is conceivable that KIBRA might function as a regulator of the degree to which a particular spine, dendrite segment, or neuron is able to stabilize new input signal information. Interestingly in this context, KIBRA overexpressed in mature primary neurons is unevenly distributed to individual dendritic spines, suggesting a preferential targeting mechanism (Supporting Information 10). While the mode of regulation of KIBRA levels or its translocation is unclear at present, it has already been shown that KIBRA can be regulated at the transcriptional level in individual neurons (Corneveaux *et al.* 2008). Our model complements existing theories on how PKMζ levels are maintained at spines for long time periods by positive feedback loops through which active PKMζ enhances its own translation by relief of a translational block (Sacktor 2011). Such a self-sustaining regulation is postulated to lead to a switch-like behavior stabilizing the activated state of the system after a critical threshold level has been reached. Depending on the way KIBRA itself is regulated, local KIBRA levels could either set the threshold of PKMζ activity required to enter the positive feedback loop leading to self-sustained activity, or act as a second component in the molecular decision process on which spines to enhance functionally.

Our data show a clear link between KIBRA levels and memory performance, a finding which could potentially be exploited clinically to counteract memory loss in human patients, e.g. by upregulating KIBRA pharmacologically. Moreover, the proteasomal degradation of PKMζ could be targeted pharmacologically, either by small molecules that inhibit proteasomal targeting of PKMζ, or by a peptidic approach using the defined binding motif within the KIBRA protein.

Supplementary Material

Refer to Web version on PubMed Central for supplementary material.

Acknowledgments

We thank Ulrike Bolz, Armin Keller, Frank Herzog, Barbara Kurpiers, Gerhard Rimner, Paul Ruf, Heike Boehli, Simone Hoppe, Vera Sonntag-Buck, Verena Kamuf-Schenk, Wolf Berger, Melanie Motsch, Joanna Schwammel, Karin Herbster, Maren Probst, Elisabeth Janesch, Karin Wacker and Nina Meyer for technical help. We for thank Friederike Kirsch for additional immunohistochemistry, and Ralph Müller for behavioural tests technical setups.

We thank Oliver Wafzig and Rico Laage for discussions. This work was supported in part by a grant from the NIH National Institute of Neurological Disorders and Stroke (NS059873 to MJH) and from the Deutsche Forschungsgemeinschaft (DFG PA483/14-2 to JK and HP). Conflict of interest statement: Several of the authors are employees of SYGNIS Bioscience. Several of the authors are inventors on patent applications covering part of the presented data.

References

Balendran A, Biondi RM, Cheung PC, Casamayor A, Deak M, Alessi DR. A 3-phosphoinositide-dependent protein kinase-1 (PDK1) docking site is required for the phosphorylation of protein kinase Czeta (PKCzeta) and PKC-related kinase 2 by PDK1. J Biol Chem. 2000; 275:20806–20813. [PubMed: 10764742]

Büther K, Plaas C, Barnekow A, Kremerskothen J. KIBRA is a novel substrate for protein kinase Czeta. Biochem Biophys Res Commun. 2004; 317:703–707. [PubMed: 15081397]

Corneveaux JJ, Liang WS, Reiman EM, et al. Evidence for an association between KIBRA and late-onset Alzheimer's disease. Neurobiol Aging. 2008

Franich NR, Fitzsimons HL, Fong DM, Klugmann M, During MJ, Young D. AAV vector-mediated RNAi of mutant huntingtin expression is neuroprotective in a novel genetic rat model of Huntington's disease. Mol Ther. 2008; 16:947–956. [PubMed: 18388917]

Frankland PW, Josselyn SA. Neuroscience: Memory and the single molecule. Nature. 2013; 493:312–313. [PubMed: 23283170]

Glanzman DL. PKM and the maintenance of memory. F1000 Biol Rep. 2013; 5:4. [PubMed: 23413372]

Hernandez AI, Blace N, Crary JF, Serrano PA, Leitges M, Libien JM, Weinstein G, Tcherapanov A, Sacktor TC. Protein kinase M zeta synthesis from a brain mRNA encoding an independent protein kinase C zeta catalytic domain. Implications for the molecular mechanism of memory. J Biol Chem. 2003; 278:40305–40316. [PubMed: 12857744]

Hongpaisan J, Xu C, Sen A, Nelson TJ, Alkon DL. PKC activation during training restores mushroom spine synapses and memory in the aged rat. Neurobiology of disease. 2013; 55:44–62. [PubMed: 23545166]

Johannsen S, Duning K, Pavenstadt H, Kremerskothen J, Boeckers TM. Temporal-spatial expression and novel biochemical properties of the memory-related protein KIBRA. Neuroscience. 2008; 155:1165–1173. [PubMed: 18672031]

Kelly MT, Crary JF, Sacktor TC. Regulation of protein kinase Mzeta synthesis by multiple kinases in long-term potentiation. J Neurosci. 2007; 27:3439–3444. [PubMed: 17392460]

Kilkenny C, Browne W, Cuthill IC, Emerson M, Altman DG. National Centre for the Replacement, R. and Reduction of Amimals in, R. Animal research: reporting in vivo experiments--the ARRIVE guidelines. Journal of cerebral blood flow and metabolism: official journal of the International Society of Cerebral Blood Flow and Metabolism. 2011; 31:991–993. [PubMed: 21206507]

Kilkenny C, Browne WJ, Cuthill IC, Emerson M, Altman DG. Improving bioscience research reporting: the ARRIVE guidelines for reporting animal research. PLoS Biol. 2010; 8:e1000412. [PubMed: 20613859]

Klugmann M, Symes CW, Leichtlein CB, Klaussner BK, Dunning J, Fong D, Young D, During MJ. AAV-mediated hippocampal expression of short and long Homer 1 proteins differentially affect cognition and seizure activity in adult rats. Mol Cell Neurosci. 2005; 28:347–360. [PubMed: 15691715]

Le Good JA, Ziegler WH, Parekh DB, Alessi DR, Cohen P, Parker PJ. Protein kinase C isotypes controlled by phosphoinositide 3-kinase through the protein kinase PDK1. Science. 1998; 281:2042–2045. [PubMed: 9748166]

Lee AM, Kanter BR, Wang D, et al. Prkcz null mice show normal learning and memory. Nature. 2013; 493:416–419. [PubMed: 23283171]

Lisman J. Memory erasure by very high concentrations of ZIP may not be due to PKM-zeta. Hippocampus. 2011; 22:648–649. [PubMed: 21956821]

Makuch L, Volk L, Anggono V, et al. Regulation of AMPA receptor function by the human memory-associated gene KIBRA. Neuron. 2011; 71:1022–1029. [PubMed: 21943600]

Migues PV, Hardt O, Wu DC, Gamache K, Sacktor TC, Wang YT, Nader K. PKMzeta maintains memories by regulating GluR2-dependent AMPA receptor trafficking. Nat Neurosci. 2010; 13:630–634. [PubMed: 20383136]

Milnik A, Heck A, Vogler C, Heinze HJ, de Quervain DJ, Papassotiropoulos A. Association of KIBRA with episodic and working memory: a meta-analysis. Am J Med Genet B Neuropsychiatr Genet. 2012; 159B:958–969. [PubMed: 23065961]

Muslimov IA, Nimmrich V, Hernandez AI, Tcherepanov A, Sacktor TC, Tiedge H. Dendritic transport and localization of protein kinase Mzeta mRNA: implications for molecular memory consolidation. J Biol Chem. 2004; 279:52613–52622. [PubMed: 15371429]

Osten P, Valsamis L, Harris A, Sacktor TC. Protein synthesis-dependent formation of protein kinase Mzeta in long-term potentiation. J Neurosci. 1996; 16:2444–2451. [PubMed: 8786421]

Papassotiropoulos A, Stephan DA, Huentelman MJ, et al. Common Kibra alleles are associated with human memory performance. Science. 2006; 314:475–478. [PubMed: 17053149]

Sacktor TC. PKMzeta, LTP maintenance, and the dynamic molecular biology of memory storage. Prog Brain Res. 2008; 169:27–40. [PubMed: 18394466]

Sacktor TC. How does PKMzeta maintain long-term memory? Nature reviews. 2010; 12:9–15.

Sacktor TC. How does PKMzeta maintain long-term memory? Nat Rev Neurosci. 2011; 12:9–15. [PubMed: 21119699]

Sacktor TC, Osten P, Valsamis H, Jiang X, Naik MU, Sublette E. Persistent activation of the zeta isoform of protein kinase C in the maintenance of long-term potentiation. Proc Natl Acad Sci U S A. 1993; 90:8342–8346. [PubMed: 8378304]

Schneider A, Huentelman MJ, Kremerskothen J, Duning K, Spoelgen R, Nikolich K. KIBRA: A New Gateway to Learning and Memory? Front Aging Neurosci. 2010; 2:4. [PubMed: 20552044]

Serrano P, Friedman EL, Kenney J, et al. PKMzeta maintains spatial, instrumental, and classically conditioned long-term memories. PLoS Biol. 2008; 6:2698–2706. [PubMed: 19108606]

Shema R, Haramati S, Ron S, Hazvi S, Chen A, Sacktor TC, Dudai Y. Enhancement of consolidated long-term memory by overexpression of protein kinase Mzeta in the neocortex. Science. 2011; 331:1207–1210. [PubMed: 21385716]

Shema R, Sacktor TC, Dudai Y. Rapid erasure of long-term memory associations in the cortex by an inhibitor of PKM zeta. Science. 2007; 317:951–953. [PubMed: 17702943]

Volk LJ, Bachman JL, Johnson R, Yu Y, Huganir RL. PKM-zeta is not required for hippocampal synaptic plasticity, learning and memory. Nature. 2013; 493:420–423. [PubMed: 23283174]

Xiao L, Chen Y, Ji M, Dong J. KIBRA regulates Hippo signaling activity via interactions with large tumor suppressor kinases. J Biol Chem. 2011; 286:7788–7796. [PubMed: 21233212]

Yao Y, Kelly MT, Sajikumar S, Serrano P, Tian D, Bergold PJ, Frey JU, Sacktor TC. PKM zeta maintains late long-term potentiation by N-ethylmaleimide-sensitive factor/GluR2-dependent trafficking of postsynaptic AMPA receptors. J Neurosci. 2008; 28:7820–7827. [PubMed: 18667614]

Yoshihama Y, Hirai T, Ohtsuka T, Chida K. KIBRA Co-localizes with protein kinase Mzeta (PKMzeta) in the mouse hippocampus. Biosci Biotechnol Biochem. 2009; 73:147–151. [PubMed: 19129633]

Zeng Y, Cullen BR. Structural requirements for pre-microRNA binding and nuclear export by Exportin 5. Nucleic Acids Res. 2004; 32:4776–4785. [PubMed: 15356295]

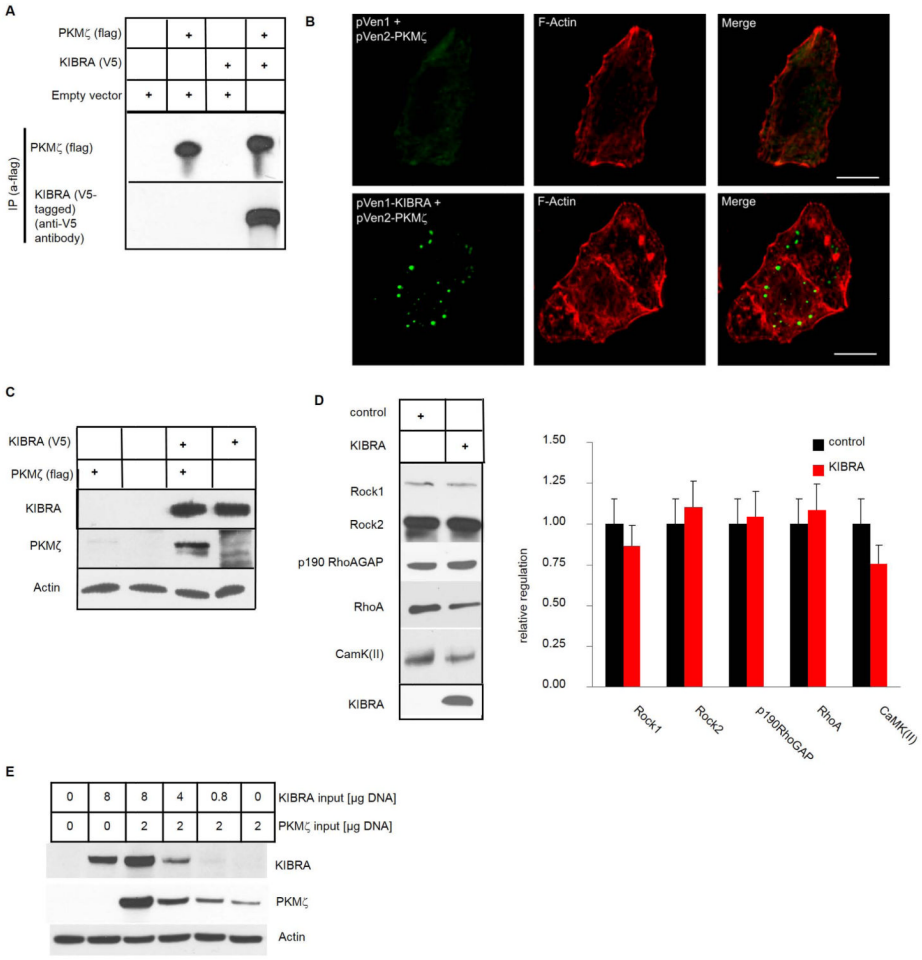

Figure 1. KIBRA binds to PKMζ and elevates cellular protein levels of the kinase

(**A**) Co-immunoprecipitation of V5-tagged KIBRA and Flag-tagged PKMζ from transfected COS1-cells with an αFlag antibody demonstrates strong interaction of both proteins. (**B**) Fluorescence complementation assay confirms interaction in intact cells. HeLa cells were co-transfected with KIBRA and PKMζ fused to the N- or C-terminal half of the Venus fluorigenic protein, respectively. F-actin was counterstained with Alexa594-conjugated phalloidin. Whereas expression of the N-terminal half of Venus with the C-terminal Venus-PKMζ fusion results in a weak and diffuse background staining, strong fluorescence signals were observed in cells cotransfected with the KIBRA-N-terminal Venus and the C-terminal Venus-PKMζ fusion indicating tight spatial interaction of both proteins. Scale bar: 10 μm. (**C**) Presence of KIBRA strongly increases detectable protein amounts of PKMζ in transfected COS1-cells. PKMζ expressed alone results in a very weak band detected by Western blot, while co-expression with KIBRA strongly enhances this signal. (**D**) Levels of several other proteins including kinases expressed in COS1 cells remain unchanged by co-expression of KIBRA, indicating the relative specificity of the observed effect to PKMζ (left, exemplary Western blots; right, quantifications from three independent experiments normalized to actin). (**E**) PKMζ protein levels are correlated directly to the amount of KIBRA present in cells. Constant amounts of PKMζ expression constructs were transfected into COS1 cells with varying amounts of KIBRA plasmids.

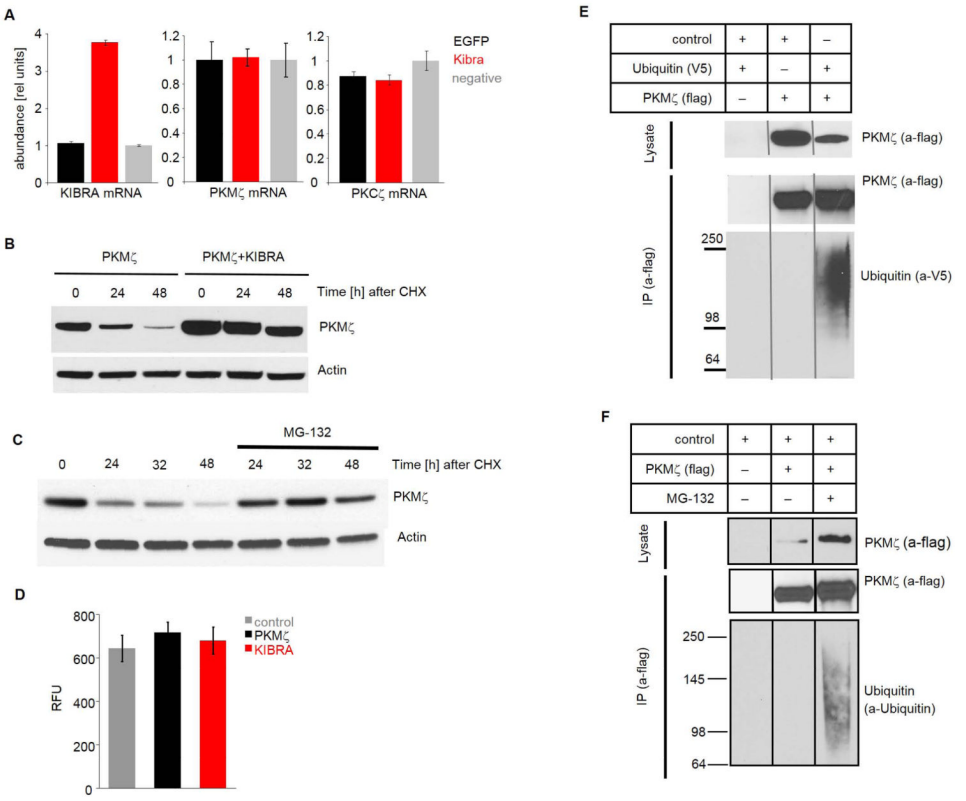

Figure 2. PKMζ is degraded by the proteasomal pathway

(**A**) Compared to untreated cells, endogenous PKMζ and PKCζ mRNA levels quantified by qPCR remain unchanged in rat primary cortical neurons infected with AAV vectors facilitating overexpression of KIBRA or EGFP. (**B**) *Left*, PKMζ protein levels decrease rapidly after treatment with the translation inhibitor cycloheximide (CHX) suggesting degradation of the kinase. *Right*, Co-expression of KIBRA blocks this degradation. CHX was added to culture medium 24 hours after transfection with expression constructs. (**C**) CHX-induced PKMζ protein degradation is abolished in COS1 cells after application of the proteasome inhibitor MG-132. (**D**) KIBRA presence has no influence on general proteasome activity as determined by a fluorigenic assay. COS1 cells were transfected with respective constructs, and harvested after 2 d. A proteasomal substrate (LLVY-7-Amino-4-methylcoumarin (AMC)) was added to the cell lysate, and presence of the free AMC fluorophore was quantified. (**E**) Ubiquitinylation of PKMζ was demonstrated by immunoprecipitation of PKMζ and subsequent detection of a co-expressed V5-tagged ubiquitin. (**F**) To demonstrate ubiquitinylation of PKMζ by endogenous ubiquitin, degradation of PKMζ was blocked by the proteasome inhibitor MG-132, allowing accumulation of the ubiquitinylated protein. PKMζ was immunoprecipitated, and ubiquitin detected by a specific antibody.

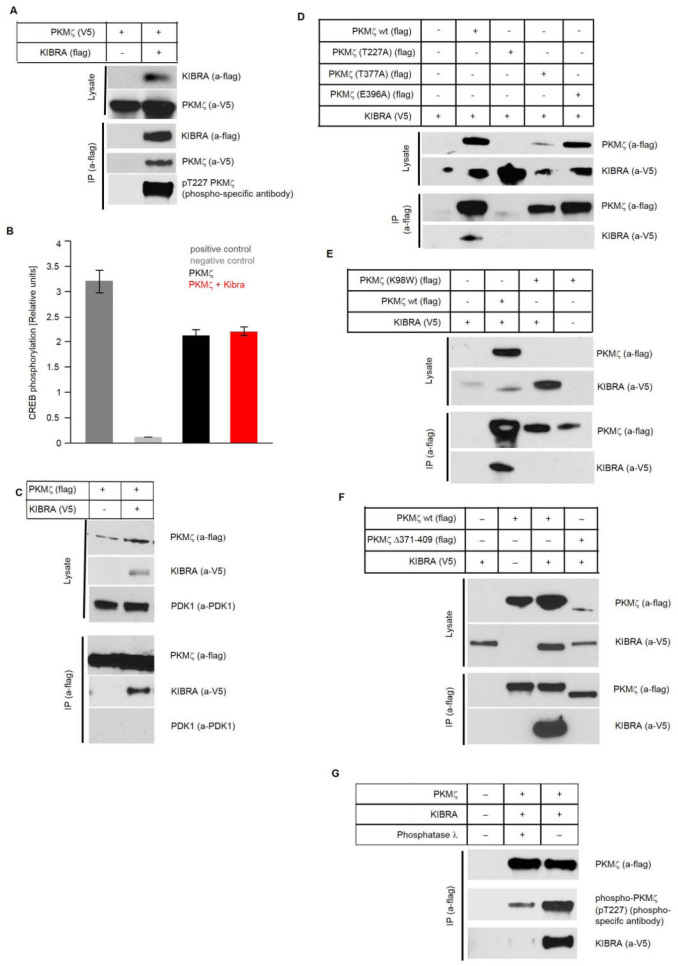

Figure 3. KIBRA binds only functional PKMζ, and PKMζ is active after binding to KIBRA

(**A**) PKMζ bound to KIBRA is phosphorylated at the activation loop threonine. Flag-KIBRA and V5-PKMζ were co-expressed in COS1 cells, co-immunoprecipitated with αFlag-beads, and PKMζ detected both by a V5-antibody, and a T227 phosphorylation-specific antibody. (**B**) CREB peptide phosphorylation assay of either commercially available PKCζ (positive control) or PKMζ immunoprecipitated from COS1 cells when expressed alone or in the presence of KIBRA. Kinase activity in the presence of KIBRA is not altered (red bar) (**C**), PDK1 is not contained in the complex of KIBRA and PKMζ. KIBRA and PKMζ were overexpressed in COS1 cells. While KIBRA was co-immunoprecipitated by an antibody against the tagged PKMζ, endogenous PDK1 was not detectable. (**D**) Binding of KIBRA to activation site mutants of PKMζ. Co-IP of KIBRA with wt PKMζ, the T227A activation-loop mutant, the T377A mutant in the turning motif, or the E396A mutant in the hydrophobic motif using αFlag beads. None of these non-functional mutants binds KIBRA. The T227A mutant is only detectable in minute amounts, suggesting strongly enhanced degradation of this form. (**E**) Co-IP of KIBRA with an ATP-orientation site mutant of PKMζ, K98W, also demonstrates loss of KIBRA-binding capacity. Detectable protein amounts of this mutant are also strongly decreased compared to the wt form of PKMζ. (**F**) Co-IP of KIBRA with the PKMζ Δ371-409 deletion construct lacking the C-terminal hydrophobic motif essential for the initial activation step of PDK1 binding. This mutant is also only weakly expressed, and does not interact with KIBRA anymore. (**G**) PKMζ and KIBRA were expressed separately, immunoprecipitated, and PKMζ was treated with

phosphatase λ. Proteins were then allowed to interact, and interaction shown by Co-IP with an antibody against flag-tagged PKMζ. Only the phosphorylated kinase is able to stably interact with KIBRA.

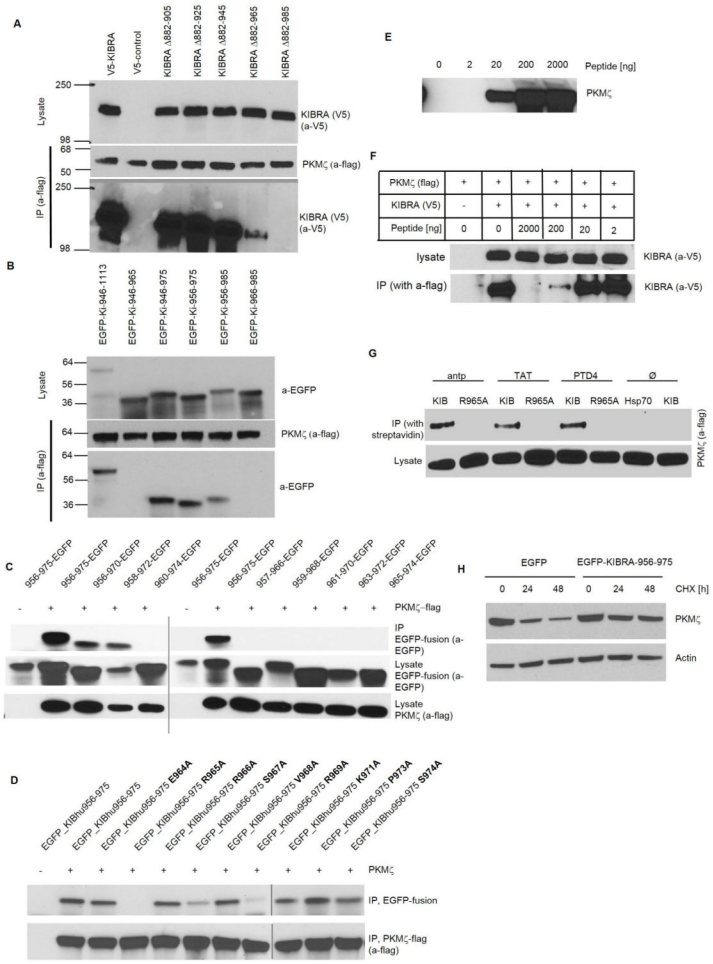

Figure 4. Binding and protection of PKMζ is dependent on a short motif near the KIBRA C-terminus

(**A**) Series of KIBRA deletion constructs for fine-mapping of the interaction site with PKMζ. Starting from aa 882, increasing 20aa stretches of KIBRA were deleted and constructs were tested for interaction with FLAG-tagged PKMζ. Very weak interaction was observed for Δ882-965, while Δ882-985 failed to interact at all, suggesting that the interaction site lies between aa946 and 985. (**B**) The region between position 946 and 985 was investigated in a reverse approach by fusing overlapping stretches of 20 or 30 amino acids to EGFP and testing for PKMζ-binding by co-immunoprecipitation. The data suggest that the binding motif lies between aa956 and 975, and that this stretch is sufficient to mediate binding. (**C**) Further deletion mapping indicates that the absolute minimal binding motif is from position 958 to 970. Only peptide fusions 956-970 and 958-972 are able to bind PKMζ, indicating that the minimal sequence required for binding is amino acids 958 – 970. However, the interaction efficiency seems to drop with both short sequences in contrast to the 20mer. (**D**) Alanine mutation scan. PKMζ-flag expression constructs were co-transfected with EGFP-fusion constructs containing the 956-975 PKMζ binding motif. Amino acids from position 964 to 974 were mutated to Alanine. The Arginine at position 965 is absolutely essential for binding. (**E**) A synthetic biotin-labeled peptide containing the binding motif (position 948-978 (DSSTLSKKPPFVRNSLERRSVRMKRPSPPPQ)) is able to bind PKMζ expressed in COS cells as shown by co-immunoprecipitation using Streptavidin beads. (**F**) The synthetic peptide 948-978 is able to disrupt a preformed KIBRA- PKMζ complex. Increasing concentrations of the peptide were added to COS-lysates co-expressing KIBRA

and FLAG- PKMζ before pull-down with anti-FLAG beads. IC50 in this assay is estimated to be around 60 nM. (**G**) A CPP-peptide fused to the PKMζ binding motif is able to penetrate cells, and bind to PKMζ inside cells. Shown is a co-immunoprecipitation with streptavidin using different biotinylated CPP motifs. Example for antennapedia: RQIKIWFQNRRMKWKK-PPFVRNSLE(R/A)RSVRMKRPSSK. (**H**) The 20-amino acid binding motif is sufficient to mediate PKMζ stability increase. Shown are PKMζ levels after addition of CHX with co-expression of the EGFP-KIBRA-956-975 construct or an EGFP control vector.

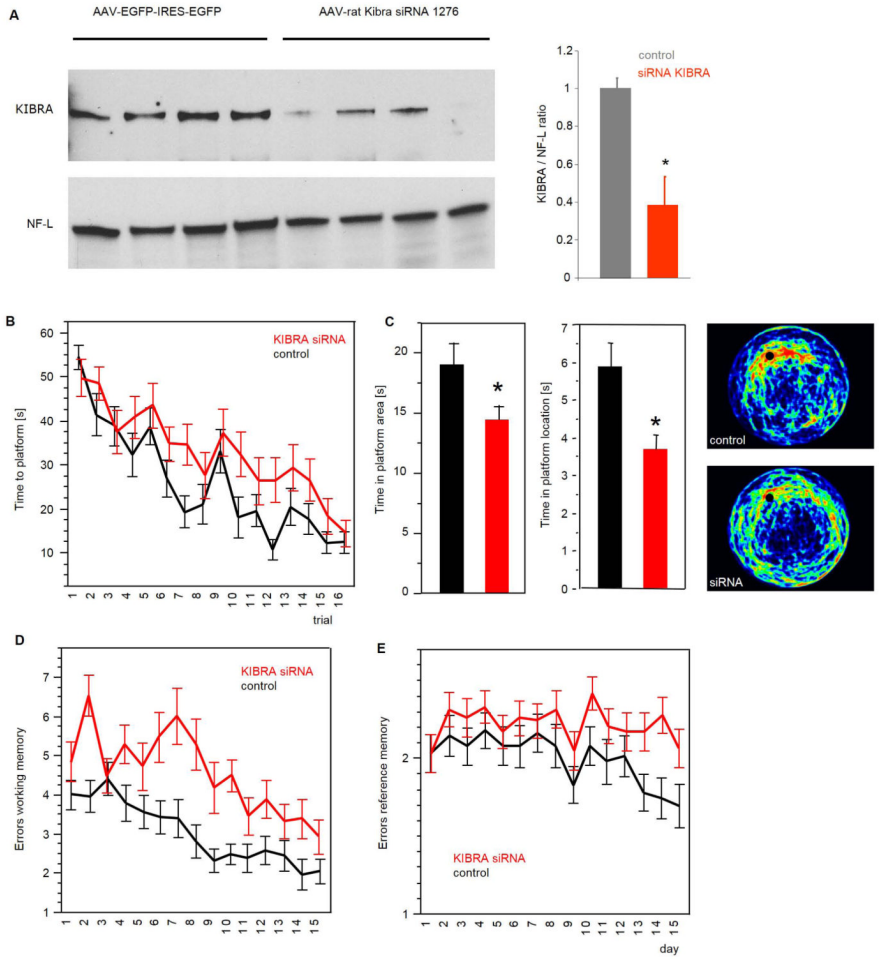

Figure 5. Knock-down or deletion of KIBRA results in spatial memory deficits

(**A)** In vivo knock-down of KIBRA in the rat hippocampus shown by Western blot and quantification of bands. For quantification, bands were densitometrized and normalized to neurofilament light chain (NF-L). KIBRA levels were decreased by 60%. (**B**) Acquisition in the Morris Water Maze over 16 trials is similar between groups with a slight disadvantage for the knock-down animals. Starting position is varied in a pseudorandom manner between four entry sites. (n=20 for control, n=19 for KIBRA knock-down). (**C**) In the probe trial, KIBRA knock-downs are significantly inferior to controls in recalling platform location both for the larger platform area, as well as for the prior platform location ($p<0.05$). This is visualized in a frequency density heat map (color coding from red to yellow to green to blue to black with red indicating the highest probability of location and black the lowest probability of location). (**D**) Analysis of working memory errors in the radial 8-arm maze reveals a difference in offset of the learning curves indicating a principally inferior learning strategy in the knock-downs ($p<0.05$ by regression analysis), while the slopes of the curves are not significantly different. (**E**) Reference memory error reduction over 15 days is significantly inferior to controls ($p<0.05$ by regression analysis).

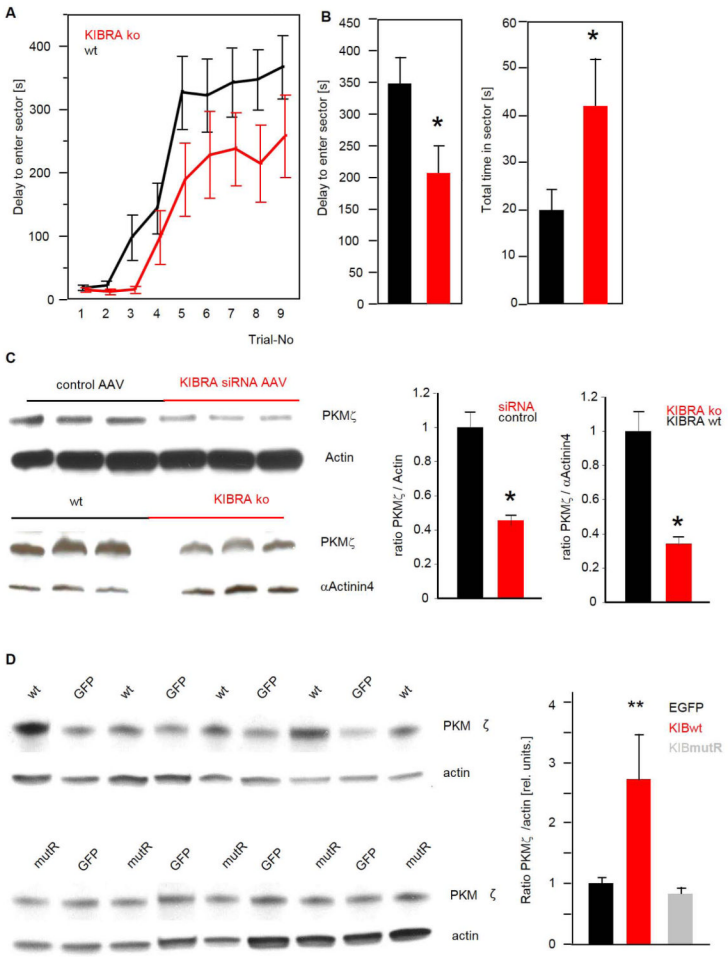

Figure 6. KIBRA knock-out mice show spatial memory deficits

(**A,B**) KIBRA KO mice (KIBRA ko, n=15; wt controls, n=19) were subjected to an active place avoidance paradigm where animals were trained to avoid a predefined sector of a rotating disc. Absence of KIBRA resulted in a significantly worse acquisition of the task (**A**), and in reduced recall of the sector location as evidenced by both entry latency (**B**, left panel), and time spent in the previously shock-associated sector (**B**, right panel) 24 h after the last training session. (**C**) Quantification of PKMζ protein in the hippocampus of KIBRA knock-down rats and KIBRA KO mice reveals significantly reduced PKMζ levels (both $p<0.05$). (**D**) Quantification of PKMζ protein in the hippocampus of rats infected with an AAV-virus expressing an EGFP-PKMζ-binding peptide, either the wt form or the R965A mutant, or EGFP only. PKMζ levels in rats infected with the wt peptide sequence show clearly elevated PKMζ levels. Quantification of PKMζ/Actin ratios on the right, the difference is significant ($p>0.01$).